

SEISMIC FRAGILITY FUNCTION FOR SINGLE STOREY MASONRY WALL RC BUILDING IN PADANG CITY, INDONESIA

*Eka Juliafad¹, and Hideomi Gokon²

¹Faculty of Engineering, Universitas Negeri Padang, Indonesia; ² Japan Advanced Institute of Science and Technology, Japan

*Corresponding Author, Received: 16 Feb. 2022, Revised: 10 March 2022, Accepted: 02 April 2022

ABSTRACT: Historical earthquakes in Indonesia show that low storey Reinforced Concrete with masonry wall buildings is vulnerable under seismic load. However, an adequate fragility function is suggested as a potential seismic assessment tool for RC buildings based on the actual condition of the existing structures. Therefore, this study aims to develop the fragility function for a typical low-storey RC building with a masonry wall in Padang City, Indonesia, based on the actual condition of the existing structures. The development of the fragility function used an analytical technique by incorporating the Applied Element Method (AEM) and Incremental Dynamic Analysis (IDA). AEM enables high accuracy of damage observation to the no-damage structures till the collapse stage. The damage stages at every PGA increment were compiled to obtain the cumulative probability. The log-normal distribution was used to derive the fragility function and create a curve. The developed fragility curve showed that at 0.3g PGA, the damage ratio of buildings sustained by slight, moderate, heavy dilapidation were 0.24, 0.54, and 0.92, respectively. The obtained fragility function to the damage ratio was validated based on the actual damage record from the 2009 West Sumatra Earthquake (2009 WSE). The comparison showed that the damage ratio obtained from the developed fragility function is close to the actual dilapidation from the 2009 West Sumatra Earthquake. Hence, the developed fragility function is potentially used as an assessment tool to predict the damage due to the Mega-Earthquake incident.

Keywords: Earthquake, Fragility, Reinforced Concrete, Masonry Wall, Damage Probability

1. INTRODUCTION

Indonesia lies on the "ring of fire" with one of the highest levels of seismic activity with high occurrences of fatality and building damage over a long history of earthquake events [1]. At the same time, Indonesia is still dealing with economic problems for low-middle income families and a lack of trained staff at the local level [2]. Thus, reducing the price of construction is prioritized over quality such that RC building construction is affected [3].

On September 30, 2009, in Padang City, a strong earthquake that occurred showed that RC buildings with masonry walls are vulnerable to destruction. The damages were varied from minor to total collapse. The field study showed that many buildings suffered significant cracking in masonry-infill and out-of-plane failure structures. The research found that the failure due to the plastic hinge was predominant at the top and bottoms of the column [4]. The recent 2018 Lombok earthquake also showed that the performance of RC buildings with masonry walls, especially those with low-rise ones, is poor under seismic load. The Indonesia disaster agency (BNPB) reported that 2337 housing had suffered extensive damage, 5909 moderate, and 6736 slights.

The significant damage to housing in Indonesia made from reinforced concrete frames, and

masonry walls showed the need for assessment of the performance subjected to seismic load [5]. Therefore, it is pertinent to evaluate the existing buildings circumspectly due to their quality uniqueness. However, this technique is not always feasible when the building inventory is enormous. An alternative to a massive building assessment is the fragility analysis. This analysis provides information on the probability of exceedance of predefined performance under different earthquake intensities. The results obtained from the fragility curves provide convenient seismic assessment tools for buildings with other structural characteristics [6-8].

Some fragility functions have been developed for seismic assessment tools in Indonesia. However, most of the available fragility functions used the empirical method, which provides the damage information based on one-time earthquake events. Meanwhile, the performance of the undamaged structure is kept unknown for a different or future earthquake incident. Some studies developed fragility functions for RC buildings based on analytical methods. However, consideration towards the actual condition seems to be neglected and yet validated with the recorded damage of previous earthquake incidents. Hence, the fragility functions validated with actual damage data are presently unavailable. This study aims to develop a

fragility function for low-rise RC buildings with masonry walls in Indonesia as the most damaged structure due to earthquake hazards. Moreover, it is based on the actual condition and validated with the recorded damage from a previous earthquake event.

2. RESEARCH SIGNIFICANCE

Based on the actual building's condition, this study aims to provide a fragility function for low-rise RC structures with masonry walls in Padang City, Indonesia. It also shows the approach of damaged justification based on Applied Elemental analysis. This research provides a fragility curve that has been validated with actual damage data from the previous earthquake, which is essential to calculate reliable damage probability for typical single-story RC buildings subjected to Indonesia's earthquake. It is also used to predict the damage to the most populated buildings and other mitigation efforts.

3. METHODS

This study uses the analytical method to create the fragility function of the typical RC buildings with a masonry wall (Fig 1). The step of the research methodology is represented in Fig 2.

3.1 Determination of Building Type

Juliafad et al. found that RC structures cover more than 85% building population in Padang City as a study area in Indonesia [9]. Hence, the numerical model used the one-story RC building with masonry walls.

3.2. Geometry of Numerical Model

The actual geometry was measured, including the total and inter-story height, layout, opening, and structural element dimension using a laser distance meter with 1 mm accuracy dan tape measurement.

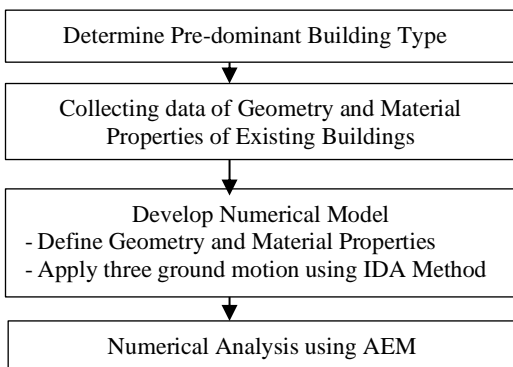


Fig.2 Research Methodology

A cross-section of structural elements was obtained, and the location of the main bars and stirrups using a rebar-locator that directly measures the steel diameter on the existing RC building.

A building model was developed using the Applied Elemental Model (AEM) provided by Extreme Loading Structure (ELS). Fig. 2 shows the layout and the facade of one of the selected buildings. This typical building uses a reinforced concrete frame with a masonry wall. Masonry walls usually are made from locally available red brick with mortar joint (1 cement: 4 sand).

The masonry wall is used to be covered with plaster-based mortar for architectural needs. The concrete and brick strength used for the numerical model was selected based on the investigation of concrete and brick from existing buildings in Padang City provided by Juliafad et al. (2018) [10].



Fig.1 Numerical Model of Typical Building

Table 1 Material Properties

Cross Section	Column	Beam
Dimension (mm)	150x150	150x180
Main Bars	4P10	4P8
Stirrups	P8-160	P8-160
Actual diameter (mm)	9.67	7.42
fy[kg/mm ²]	24.89	22.06
fu/fy	1.4	1.76

3.3. Building's Material Properties

The numerical model in this study used the predominant value of material strength from existing RC buildings with masonry walls in Padang City (Table 1).

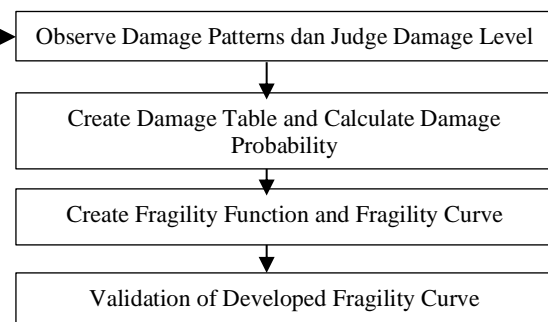


Table 2 Material Properties

Input Material	Concrete	Mortar Cement	Red Brick
f'_c [MPa]	17.5	2.017	0.8
f_t [MPa]	2.9	0.0217	0.08
E[MPa]	19492.3	79.74	13.14
G[MPa]	8121.8	33.225	7.57
f_v [MPa]	2.236	0.504	0.019

Table 2 presents the detailed properties of mortar and red brick from the existing buildings. The tensile strength parameters were calculated, as well as the young's and shear modulus using Eq. (1), (2), and (3), respectively

$$f_t = 0.7\sqrt{f'_c} \quad (1)$$

$$E = 4700\sqrt{f'_c} \quad (2)$$

$$G = \frac{E}{1+\nu} \quad (3)$$

When f'_c is compression strength, E is young's modulus, G is the shear modulus, ν is the Poisson ratio.

3.3. Earthquake Loading for Numerical Model

This study used 3(three) actual ground motion records with different magnitudes and frequencies (Table 3). This is to ensure the building performances and damages are represented in a wide range of earthquake characteristics. Those ground motion records are Kobe, Loma Prieta, and El Centro earthquakes.

3.4. Numerical Analysis and Fragility Function Derivation

Previous research used the Finite Element Method (FEM) as the numerical tool. FEM simulation is limited in performing the actual damage patterns of masonry walls, especially out of plane failure. The features of the tools that give a better damage description are essential to justify the numerical model's destruction level, especially for buildings with masonry walls. Hence, this research used the Applied Element Method (AEM) to show the damage to the buildings from no dilapidation to a collapsed state. AEM shows the out-of-plane

failure of the masonry wall and the crack patterns from slight damage to a total collapse state [11–13].

This study utilizes the Incremental Dynamic Analysis (IDA) method to apply ground motion records to the numerical model. IDA method is a dynamic analytical technique that incrementally magnifies the ground motion records gradually till the collapse state [14–18]. Incremented loading enables the detailed observation of the damage pattern of a numerical model for every step of earthquake loading magnification from the early state (undamaged) to total collapse.

The damage level justification is a crucial step in developing the fragility function. As the AEM visually enables an accurate observation of damage patterns, the destruction description that is used should be detailed. This study used the damage description based on the table of destruction patterns for RC buildings with infill walls that were developed by Rosetto and Elnashai[19].

The method used to calculate the damage ratio is cumulative destruction probability. The derivation of the fragility function used log-normal cumulative distribution. Ramesh (2015) used a cumulative log-normal distribution function which followed the recommendation from HAZUS (2003) and other damage assessment tools [20–21]. The results showed a good correlation between the fitting fragility curve and damage probability. For structural damage, at the given PGA, the probability of an element at risk exceeding a damage level is calculated as Eq (4).

$$P[ds/PGA] = 1/2 \left[1 + \operatorname{erf} \left(\frac{(\ln PGA - \mu)/(\beta\sqrt{2})}{1} \right) \right] \quad (4)$$

Where erf is the complementary error function, μ is mean = $\ln PGA_{ds}$, PGA_{ds} is the median value of PGA at which the building reaches the threshold of

Table 3 Ground Motion Records

Ground motion	Duration (s)	Time Step		Main Period (s)	Frequency (Hz)
		Step (s)	Total data		
Kobe	40.96	0.01	4096	0.47	2.13
El Centro	50.0	0.01	4000	0.25	4
Loma Prieta	39.955	0.005	7991	0.15	6.67

the damage state d_s and β is the Standard Deviation which represents the fragility curve's dispersion [22].

To calculate the probability where the building reaches the damage state at a particular PGA (d_s /PGA), the total number of building damage was obtained at a particular state for each incremented PGA (Table 3). Subsequently, the damage ratio was calculated for slight, moderate, severe, and collapse states following the equation as Eq (5), Eq (6), Eq (7), and Eq (8), respectively.

$$a_{st} = \frac{N_{st} + N_{md} + N_{sv} + N_{cp}}{\sum N} \quad (5)$$

$$a_{md} = \frac{N_{md} + N_{sv} + N_{cp}}{\sum N} \quad (6)$$

$$a_{sv} = \frac{N_{sv} + N_{cp}}{\sum N} \quad (7)$$

$$a_{cp} = \frac{N_{cp}}{\sum N} \quad (8)$$

Where a_{st} is the ratio of slight damage, a_{md} is the ratio of medium damage, a_{sv} is severe damage ratio, and a_{cp} is collapse damage ratio, while N is the number of building suffering damage.

$$PGA_{d_s} = PGA_{d_{s_{i+1}}} - (\Delta_{PGA}) \times \frac{(a_{d_s/PGA_{d_{s_{i+1}}}} - (\frac{\Delta_{PGA}}{2}))}{a_{d_s/PGA_{d_{s_{i+1}}}} - a_{d_s/PGA_{d_{s_i}}}} \quad (9)$$

$$\Delta_{PGA} = PGA_{d_{s_{i+1}}} - PGA_{d_{s_i}} \quad (10)$$

$$\mu = \ln PGA_{d_s} \quad (11)$$

$$\beta = \sqrt{\frac{\sum \{f_i \cdot \ln(x_i - \bar{x})^2\}}{\sum f_i}} \quad (12)$$

$$f_i = a_{i_{PGA_{d_s}}} \quad (13)$$

$$x_i = PGA_{i_{PGA_{d_s}}} \quad (14)$$

$$\bar{x} = \frac{(\ln_{PGA_{d_s}} + \sum x_i f_i / \sum f_i)}{2}$$

After finding the damage ratio, the median value of threshold PGA was calculated using (Eq (9)), the mean value using (Eq (10)), the standard deviation using (Eq (11)), and the probability of the damages that occurs at PGA (Eq (4))

4. RESULTS AND DISCUSSION

4.1 Numerical Simulation Results

A total of 390 numerical simulations were conducted to cover a wide range of incremented ground motion records showing a whole level of damage. The damage patterns of the buildings were observed through the visualization of the crack propagation, deformed shape, and extent of the destruction. The numerical model subjected to El-Centro Earthquake starts to suffer slight damage at 0.1g, where the crack begins to appear at the corner of the opening (Cracks are identifiable through the black line on the brick wall). In contrast, the structural elements (column and beam) do not damage or crack (Fig. 4(a)).

Moderate damage occurred at 0.3g PGA, where the diagonal cracks are extended throughout the wall, from the corner top to the bottom. Some part of the masonry wall also falls from the top of the opening (window). Some cracks start to occur at structural elements (beam) or the joint area (Fig.4(b)). Fig.4(c) shows the damage patterns of RC building type A at 0.4g. At this stage, many of the infill walls suffered the plan and heavier damage. Although many of the walls were fallen, the structural elements are still attached. However, the cracks in the structural elements are extending; hence, the damage rate is judged as extensive dilapidation at this level. Finally, the earthquake loading was magnified to 0.7g, and the building started to collapse (Fig. 4(d)).

Table 3 compiled each damage level as categorized into no damage (N), slight (S), moderate (M), extensive (E), and collapse (C) for each PGA incremental. These were then calculated as cumulative damage probability (Table 4)

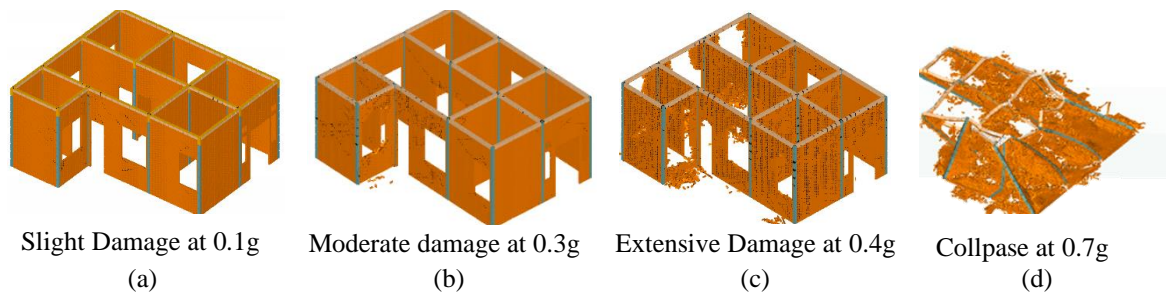


Fig.4 Damage Patterns of Numerical Model subjected to El-Centro Earthquake

Table 3 Damage Level for 1 story RC building type in Padang

Damage Level	Peak Ground Acceleration (g)												
	0.05	0.1	0.2	0.3	0.4	0.5	0.6	0.7	0.8	0.9	1	1.1	1.2
No Damage (N)	30	10	0	0	0	0	0	0	0	0	0	0	0
Slight (S)	0	20	30	10	0	0	0	0	0	0	0	0	0
Moderate (M)	0	0	0	20	20	10	0	0	0	0	0	0	0
Extensive (E)	0	0	0	0	10	20	30	20	20	20	20	0	0
Collapse (C)	0	0	0	0	0	0	0	10	10	10	10	30	30
Total (ΣN)	30	30	30	30	30	30	30	30	30	30	30	30	30

Table 4 Cumulative Probability Damage for one story RC building type in Padang

DS	Peak Ground Accelerations (g)											
	0.1	0.2	0.3	0.4	0.5	0.6	0.7	0.8	0.9	1	1.1	1.2
S	0.67	1.00	1.00	1.00	1.00	1.00	1.00	1.00	1.00	1.0	1.0	1.0
M	0.00	0.00	0.67	1.00	1.00	1.00	1.00	1.00	1.00	1.0	1.0	1.0
E	0.00	0.00	0.00	0.33	0.67	1.00	1.00	1.00	1.00	1.0	1.0	1.0
C	0.00	0.00	0.00	0.00	0.00	0.00	0.00	0.33	0.33	0.33	1.0	1.0

4.2. Fragility Function and Fragility Curve.

The cumulative probability value for each damage state and each PGA value (Table 4) were derived by using log-normal distribution Eq (4) to obtain the value of the median (μ) and standard deviation (β) for typical low story RC building with masonry wall in Padang City for each level of damage state (Table 5)

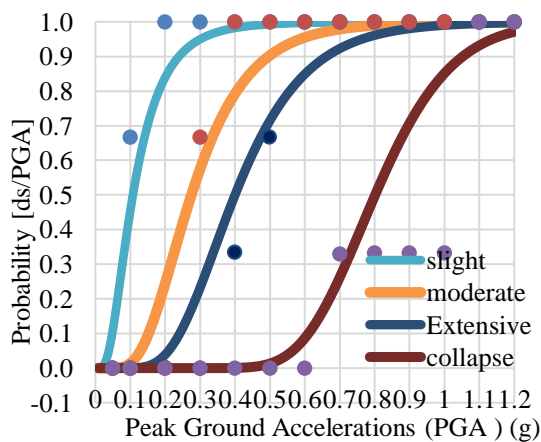


Fig.5 Fragility Curves for Typical low rise RC Building with Masonry Walls

Table 5. Median and Standard Deviation of Fragility Curve

Damage States (ds/PGA)	Median (0.5 PGA)	Mean (μ)	Standard Deviation (β)
Slight	0.108	-2.230	0.625
Moderate	0.275	-1.291	0.460
Extensive	0.400	-0.916	0.393
Complete	0.802	-0.221	0.212

Parameters obtained from functions for each level enable the creation of fragility curves (Fig. 5). The probability of a low story RC building with a

masonry wall being damaged in the future under earthquake excitation at any PGA value was calculated/predicted.

4.3. Validation of Developed Fragility Curve

Figure 7 shows the Peak Ground Acceleration (PGA) distribution map for Padang City. This PGA map was created using deterministic and probabilistic methods considering the sources of the earthquake in this area. The primary sources are the subduction area and the Semangko fault [23–24].

Table 6 shows the estimation of housing damage data in Padang City, compiled from local government offices in Padang City. The provincial government classified the building damage into 3 categories; severe or excessive, moderate or over, and slight damage. Severe damage means that the observed buildings were structurally damaged until they collapsed. In this state, the buildings were irreparable. Moderate damage means that the damages are widespread and still repairable, and slight damage means it is easily fixable.

The housing damage data for 11 sub-districts in Padang City due to the 2009 Earthquake is observed in Table 6. The damage ratio for each level of previous earthquake data was calculated using the cumulative method. This is compared with the damage ratio based on the developed fragility function for typical housings made from RC buildings with masonry walls in Padang City.

Utilizing the developed fragility function for typical RC buildings for housings in Padang City resulted in this study (Fig. 5), each damage ratio of RC building in 11 sub-districts was calculated at the average value of PGA for each sub-district.

The average damage ratio obtained from the developed fragility function was compared with the destruction ratio of the 2009 earthquake incident (Fig.6). The slight damage from the fragility function shows a higher value than the actual. The

moderate or over and severe or excessive damage levels show a good correlation with the actual destruction. The histogram of comparison between damage ratio based on the developed fragility curve and actual damage data is shown in Fig.6.

While the actual damage was based on one earthquake event, the developed fragility functions were based on some extreme earthquake ground motion and the actual conditions of the building. The damage patterns in this study have been judged strictly compared to the actual destruction level judgment. With the limitation on the field, the observer of the actual damage finds it challenging to detect the fine or small wide cracks in detail due to the insufficient experience of field inspectors, inspection timing, tool, and access to all parts of observed buildings called empirical fragility.

Hakam (2010) developed a vulnerability curve for housing in West Sumatra. The data were based on the building damage data of the 2009 Earthquake

in West Sumatra. However, the curve was based on the empirical data, which shows the actual damage on another side. Moreover, it does not show the probability of housing damage in the future for a different earthquake — the type of building addressed on the curve was also unclear and very general. The provided information is also limited to severe damage only[25–26].

Irsyam et al. derived fragility curves for two types of low-rise buildings that dominate the residential building population in Jakarta. The fragility curves are derived based on FEMA 154 procedures for different levels of damage (i.e., Slight, Moderate, Extensive, and Complete Damages), and the ground motion intensity is expressed regarding Peak Surface Acceleration (PSA)[26]. Unfortunately, the process of the curve derivation is not explained clearly, and the curve also seems not well fitted.

Table 6 Comparison of Damage ratio of developed fragility function with Damage Ratio of actual damage

Area	Damage Ratio based on actual damage data on the 2009 Padang Earthquake				Damage Ratio based on Developed Fragility Function		
	average PGA	Extensive or more	Moderate or over	Slight or over	Extensive Or more	Moderate or more	Slight or over
L.kilangan	0.38g	0.27	0.50	0.76	0.44	0.74	0.97
K.Tengah	0.36g	0.28	0.60	0.90	0.39	0.72	0.97
Kuranji	0.35g	0.31	0.60	0.90	0.25	0.69	0.97
P.Barat	0.31g	0.20	0.41	0.64	0.25	0.60	0.95
P.Utara	0.3g	0.23	0.50	0.77	0.23	0.57	0.95
P.Selatan	0.29g	0.28	0.56	0.89	0.20	0.54	0.94
P.Timur	0.29g	0.14	0.39	0.67	0.20	0.54	0.94
Nanggalo	0.28g	0.24	0.41	0.53	0.18	0.51	0.93
L.Begalung	0.28g	0.28	0.57	0.93	0.18	0.51	0.93
Pauh	0.25g	0.16	0.37	0.66	0.16	0.42	0.91
B.T.Kabung	0.25g	0.05	0.09	0.15	0.16	0.42	0.91
Padang City	0.30g	0.22	0.54	0.71	0.24	0.54	0.94

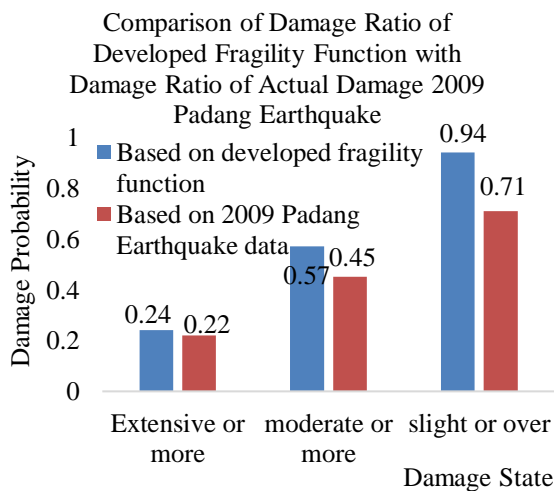


Fig. 6 Comparison of Average Damage Ratio of Developed Fragility Function and Actual Damage Building 2009 Padang Earthquake

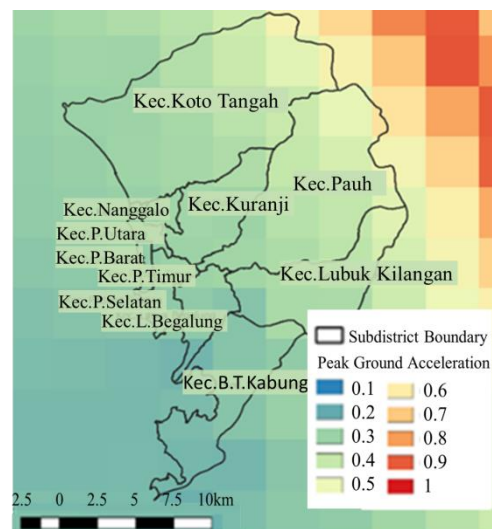


Fig. 7 Peak Ground Acceleration Map of Padang City, Indonesia.

Compared to the existing fragility or vulnerability curves, the developed fragility function has been validated, giving an accurate prediction that is utilizable by the government. Also, other stakeholders need to build a vulnerability map and disaster reduction counter-measures activities/programs.

Table 6. also compares the damage ratio of developed fragility function and actual destruction building data of the 2009 September Earthquake for 11 sub-districts in Padang City. The damage ratio between developed fragility function and actual destruction data ratio shows a good correlation.

However, some gaps were found in 3 sub-districts that were possibly due to the different conditions of the local site. The gaps were quite big at a slight damage level due to the different damage pattern observation and judgment results between the actual and the numerical study. The local, hard, or soft soil conditions affect the building performance as part of soil-structure interaction. The other factors include the difference between construction method qualities, wherein one sub-district work quality is good, and the other bad [2–3].

5. CONCLUSION

This study successfully developed an analytical fragility function for residential low-rise masonry walls RC buildings, based on the actual condition of the existing structures. The dimension and material characteristics of the numerical model were obtained from field assessment and then analyzed using the AEM. The AEM followed the building failure until the collapse stage and accurately observed the damage patterns for each intensity level. Furthermore, this study obtained the damage ratio and used the log-normal probability formula to create a fragility function.

The comparison between the average actual damage ratio of the 2009 September earthquake in Padang City and the developed fragility function showed a good correlation. The severe (or excessive) and moderate (or over) damage showed a good comparison. This comparison emphasized that the developed fragility function showed the actual performance of low-rise RC buildings in Padang City.

The Indonesian government may use the developed fragility as the seismic assessment tool to make a vulnerability map and the preparedness for earthquake disasters, especially for single-story RC buildings. In the future, it is necessary to develop seismic fragility functions for other types of buildings and consider the effects of defects that are commonly found in the existing structures.

6. ACKNOWLEDGMENTS

We appreciate the Universitas Negeri Padang for the grant aid in 2018 and 2019 and the University of Tokyo for the assistance.

7. REFERENCES

- [1] Wahyuni, E., Vulnerability Assessment of Reinforced Concrete Building Post-Earthquake, *Procedia Earth and Planetary Science*, vol. 14, no. August, pp. 76–82, 2015, doi: 10.1016/j.proeps.2015.07.087.
- [2] Juliafad, E., and Andayono, T., Study on building permit awareness in West Sumatra, Indonesia, *IOP Conf. Ser.: Earth Environ. Sci.*, vol. 708, no. 1, p. 012093, Apr. 2021, DOI: 10.1088/1755-1315/708/1/012093.
- [3] Juliafad, E., Gokon, H., and Putra, R.R., Defect Study on Single Storey Reinforced Concrete Building In West Sumatra: Before And After 2009 West Sumatra Earthquake, *Geomate*, vol. 20, no. 77, Jan. 2021, DOI: 10.21660/2020.77.ICEE03.
- [4] Wilkinson, S. M., Alarcon, J. E., Mulyani, R., Whittle, J., and Chian, S. C., Observations of damage to buildings from M w 7.6 Padang earthquake of September 30, 2009, *Nat Hazards*, vol. 63, no. 2, pp. 521–547, Sep. 2012, DOI: 10.1007/s11069-012-0164-y.
- [5] Jalayer, F., Ebrahimian, H., Miano, A., Manfredi, G., and Sezen, H., Analytical fragility assessment using unscaled ground motion records, *Earthquake Engng Struct Dyn*, vol. 46, no. 15, pp. 2639–2663, Dec. 2017, DOI: 10.1002/eqe.2922.
- [6] Cardone, D., Fragility curves and loss functions for RC structural components with smooth rebars, *Earthquakes, and Structures*, vol. 10, no. 5, pp. 1181–1212, May 2016, DOI: 10.12989/EAS.2016.10.5.1181.
- [7] Del Gaudio, C., Ricci, P., Verderame, G. M., and G. Manfredi., Development and urban-scale application of a simplified method for seismic fragility assessment of RC buildings," *Engineering Structures*, vol. 91, pp. 40–57, May 2015, doi:10.1016/j.engstruct.2015.01.03.
- [8] Rossetto, T., FRACAS: A capacity spectrum approach for seismic fragility assessment including record-to-record variability, *Engineering Structures*, vol. 125, pp. 337–348, Oct. 2016
- [9] Juliafad, E., Meguro, K., and Gokon, H., Study on The Environmental System towards The Development of Assessment Tools for Disaster Reduction of Reinforced Concrete Building due to Future Mega-Earthquake in Padang City, Indonesia, *Institute of Industrial Science The University of Tokyo*, 2017. Accessed:Feb.15,2020.Available:<https://doi.org/10.11188/seisankenkyu.69.351>

- [10] Juliafad, E., Meguro, K., and Gokon, H., Study on The Characteristic of Concrete and Brick as Construction Material for Reinforced Concrete Buildings in Indonesia, Institute of Industrial Science The University of Tokyo, November 01, 2018. Accessed: Feb. 15, 2020. Available: <https://doi.org/10.11188/seisankenkyu.70.437>
- [11] Meguro, K., and Tagel-Din, H., Applied Element Simulation of RC Structures under Cyclic Loading, *J. Struct. Eng.*, vol. 127, no. 11, pp. 1295–1305, Nov. 2001, DOI: 10.1061/(ASCE)07339445(2001)127:11(129).
- [12] Domaneschi, M., Collapse analysis of the Polcevera viaduct by the applied element method, *Engineering Structures*, vol. 214, p. 110659, Jul. 2020, DOI: 10.1016/j.engstruct.2020.110659.
- [13] Grunwald, C., Reliability of collapse simulation – Comparing finite and applied element method at different levels, *Engineering Structures*, vol. 176, pp. 265–278, Dec. 2018, doi: 10.1016/j.engstruct.2018.08.06.
- [14] Vamvatsikos, D., and Cornell, C. A., Incremental dynamic analysis, *Earthquake Engng. Struct. Dyn.*, vol. 31, no. 3, pp. 491–514, Mar. 2002, DOI: 10.1002/eqe.141.
- [15] Kaveh, A., Javadi, S. M., and Moghanni, R. M., Optimization-based record selection approach to incremental dynamic analysis and estimation of fragility curves, *Scientia Iranica*, p. 9, 2021.
- [16] Capanna, I., Cirella, R., Aloisio, A., Alaggio, R., Di Fabio, F., and Fragiacomò, M., Operational Modal Analysis, Model Update, and Fragility Curves Estimation, through Truncated Incremental Dynamic Analysis, of a Masonry Belfry, Buildings, vol. 11, no. 3, p. 120, Mar. 2021, DOI: 10.3390/buildings11030120.
- [17] Yahyapour, R., and Seyedpoor, S. M., Comparing the Seismic Behavior of Various Knee Braced Steel Frames Based on Incremental Dynamic Analysis and Development of Fragility Curves, *Int J Steel Struct*, vol. 21, no. 4, pp. 1228–1241, Aug. 2021, DOI: 10.1007/s13296-021-00501-1.
- [18] Juliafad, E., and Melinda, A. P., Assessment of Reinforced Concrete Building for Disaster Reduction Strategy in Padang City, West Sumatra, Indonesia, *MATEC Web Conf.*, vol. 258, p. 03007, 2019, doi: 10.1051/mateconf/201925803007.
- [19] Rossetto, T., and Elnashai, A., A new analytical procedure for the derivation of displacement-based vulnerability curves for populations of RC structures, *Engineering Structures*, vol. 27, no. 3, pp. 397–409, Feb. 2005, doi: 10.1016/j.engstruct.2004.11.002.
- [20] Guragain, R., Dixit, A. M., and Meguro, K., Development of Fragility Functions for Low Strength Masonry Buildings in Nepal using Applied Element Method, p. 10. At 15th world conference of earthquake engineering, Lisbon, Portugal, 2012
- [21] Kircher, C. A., Whitman, R. V., and Holmes, W. T., HAZUS Earthquake Loss Estimation Methods, *Nat. Hazards Rev.*, vol. 7, no. 2, pp. 45–59, May 2006, DOI: 10.1061/(ASCE)1527-6988(2006)7:2(45).
- [22] Janpila, A., The Optimal Method for Building Damage Fragility Curve Development, *Geomate*, vol. 18, no. 69, May 2020, DOI: 10.21660/2020.69.9192.
- [23] Haridhi, H. A., Huang, B.S., Wen, K.L., Denzema, D., Prasetyo, R. A., and Lee, C.S., A study of large earthquake sequences in the Sumatra subduction zone and its possible implications, *Terr. Atmos. Ocean. Sci.*, vol. 29, no. 6, pp. 635652, 2018, doi: 10.3319/TAO.2018.08.22.01.
- [24] Putra, R. R., Damage Investigation And Re-Analysis Of Damaged Building Affected By The Ground Motion Of The 2009 Padang Earthquake, *Geomate*, vol. 18, no. 66, Feb. 2020, DOI: 10.21660/2020.66.Icee2nd.
- [25] Hakam, A., Ismail, F., and Nur, O., Earthquake Damage – Intensity Relationship, 15th World Conference on Earthquake Engineering (15WCEE), 2012.
- [26] Irsyam, M., Development of Seismic Risk Microzonation Maps of Jakarta City, *Geotechnics for Catastrophic Flooding Events 2014*, pp. 35–47. DOI: 10.1201/b17438-6.